International Journal of Networks and Communications 2016, 6(2): 24-31
DOI: 10.5923/j.ijnc.20160602.02

Comparing Shell Mapping to Trellis Shaping as Symbol Mapping for Co-existence of next Generation PON and Current System

Yasuyuki Okumura*, Katsuyuki Fujii, Kohei Oowaki

Department of Science and Engineering, Nanzan University, Aichi, Japan

Abstract This paper describes the results of comparing shell mapping to trellis shaping in terms of symbol mapping that can improve the transmission characteristics of next generation Passive Optical Network (PON) system when co-existing with the conventional system. A mapping proposal solves one of the most critical problems; the small Euclid distance of the PSK signals in a constellation shared by OOK and PSK. The conventional system uses on-off keying (OOK) for its simplicity, while the next generation uses advanced techniques such as phase shift keying (PSK). Constellation sharing and the use of Digital Signal Processing technology can allow the next generation PON to co-exist with the conventional system, which is advantageous for the migration of the access network. Shell mapping and trellis shaping are simple and effective symbol mapping approaches for signal shaping algorithms that can maximize the symbol distance assuming the co-existence of OOK and PSK. This paper shows the operating principles of symbol mapping, and also describes the co-simulation configuration of MATLAB and OptSim used to clarify the improvement achieved by the mapping. It shows that trellis shaping improves BER more than shell mapping, and so enables smooth migration from conventional PON to the next generation.

Keywords Constellation Sharing, Next generation PON, Signal Shaping

1. Introduction

Passive optical networks (PONs) deliver not only various services such as the Internet, video, and voice at the same time, but also outstanding flexibility and scalability. In recent years, services for healthcare, education, and mobile backhaul for advanced mobile communications have also moved to optical networks. The demand for these services is spurring research into the next generation PON that should provide sufficient bandwidth and flexibility to meet the requirements. Network operators want these benefits while still operating existing access networks, so the telecom industry is interested in the incremental adoption of the next generation PON [1-9].

Several prospective candidate technologies for the next generation PON are Wavelength Division Multiple Access (WDMA), Code Division Multiple Access (CDMA), and Orthogonal Frequency Division Multiple Access (OFDMA). Although these technologies deliver large transmission capacity, they possess inherent weaknesses. As an example, WDMA uses high cost devices such as wavelength multiplexers and laser diodes of various wavelengths. To realize home use, cost-effective devices and technologies must be adopted for the next generation PON systems [10-13].

One realistic approach to the next generation PON involves the use of advanced modulation schemes such as Amplitude Shift Keying (ASK), Phase Shift Keying (PSK) and Quadrature Amplitude Modulation (QAM). These necessitate modulating the phase and amplitude of optical sub-carrier signals and the use of Digital Signal Processing (DSP). A key advantage of these modulation formats is their co-existence with the On-off Keying (OOK) signals used in the existing PON. The co-existence is realized by constellation sharing; one terminal uses the OOK (amplitude modulation) format of the existing PON while another uses an advanced (amplitude and phase modulation) modulation format [14-19]. For example, one data stream is transferred by the amplitude information of the modulation format, whereas the phase information expresses the other data stream. OOK is identical to using just the amplitude of the advanced modulation format.

Constellation sharing, however, can seriously degrade the performance of the advanced modulation format. The reason is that the OOK signal needs large extinction ratios to achieve low Bit Error Rates (BERs), but this makes it difficult to discriminate the symbols via the phase information. This paper describes a symbol mapping solution based on signal shaping, such as shell mapping and

* Corresponding author:
yokumura@nanzan-u.ac.jp (Yasuyuki Okumura)
Published online at http://journal.sapub.org/ijnc

trellis shaping. These signal shaping methods alleviate the trade-off between BER phase information in constellation sharing. This paper also describes the co-simulation configuration of MATLAB and OptSim, both of which are widely used in the design of communication technologies, used to clarify the improvement realized by the mapping proposal. Simulations show that the new mapping improves the BER of the advanced modulation format. It shows that trellis shaping improves BER more than shell mapping, and so will enable the smooth migration from the conventional PON to the next generation.

2. Constellation Sharing [14, 15]

A simplified PON model is shown in Figure 1(a), where the optical line terminator (OLT) is connected to multiple optical network units (ONUs) via a passive optical splitter. The co-existence of different types of ONUs that use different modulation formats is considered essential for network evolution. In sending the different data streams from the OLT to multiple ONUs, each data stream must suit the intended ONU. Constellation sharing uses multilevel modulation signals such as OOK+PSK, and the number of bits allocated to a symbol differs with the intended ONU. For example, in 8-star OOK+PSK, 3 bits data are allocated to each symbol; 1 bit for 2 level amplitude, and 2 bits for 4 phases, as shown in Figure 1(b). Constellation sharing enables the OLT to send different data streams using the amplitude levels and/or phase information. Figure 1(a) shows that ONU #1 classifies the data stream as OOK and so uses the amplitude level, where each symbol carries 1 bit, i.e., the conventional PON. ONU #3 captures PSK coded symbols, i.e. coding uses phase information and each symbol contains 2 bits. Each ONU separately receives the allocated data stream, assembles data frames, and determines whether the data frame contains the destination address of the ONU. If the address represents another ONU, the receiving ONU discards the data frame. In constellation sharing, the bit allocation to each ONU is variable, which provides flexible transmission capacity allocation.

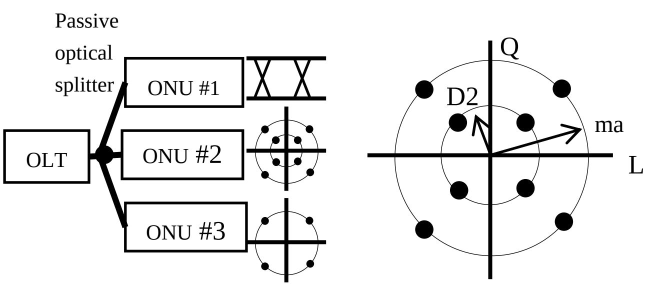

b(a) Configuration (b) Constellation

Figure 1. Constellation sharing

In OOK, extinction ratio ε must be large enough to match the BER performance of the existing PON. ε is defined by Eq. (1),

$$\varepsilon=10\log_{10}(D1/D2)^2, \quad (1)$$

where $D1$ and $D2$ are the radii of the outer and inner circles of the constellation as shown in Fig. 1(b), respectively. A large value of ε yields better BER, since the Euclidian distance is reduced when the symbols are OFF. Constellation sharing reduces the Euclidian distance of the PSK symbols and degrades the BER of the PSK signals, when the symbols are OFF, as shown in Figure 1.

3. Signal Shaping [20, 21]

Signal shaping aims to reduce the signal power without increasing the BER [20, 21]. In the conventional system design, the least average signal power is desired, since the transmit power causes crosstalk noise in the transmission line. Signal shaping efficiently controls the power by employing the well-known error correcting code. It is based on shaping the regions of the constellation, which is divided into M regions, as shown in Figure 2. Each region has equal area, i.e. the same number of symbols. Assuming the regions are numbered from s=0 to M-1, starting from the innermost one, the symbols in region s=0 bear the least power. Using the M regions of the constellation, an N-tuple of the region number with M^N possible sequences can express N consecutive symbols. Given that the data sequence of K bits is transferred, 2^K sequences with least energy can be selected from all sequences. To realize this, the symbols are selected from the innermost possible regions, i.e. the lowest region numbers.

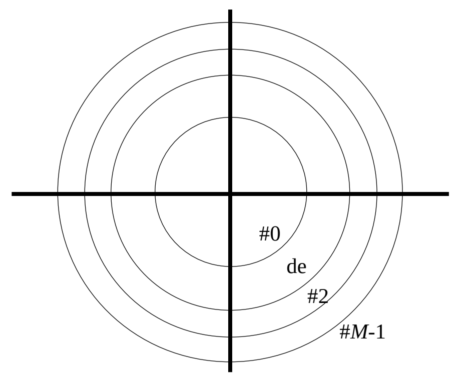

Figure 2. Partitioning the constellation into M regions

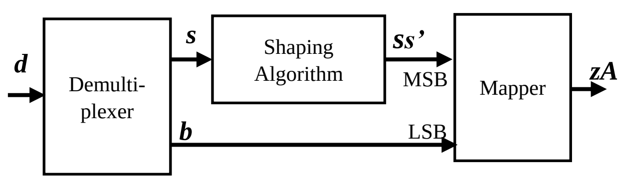

Figure 3. Signal shaping block diagram

The principles of signal shaping are described in [22]. The signal shaping block diagram is shown in Figure 3, where ***d*** is the data sequence to be transmitted. Data ***d*** is divided into ***s*** and ***b***, where ***s*** is the most significant bit (MSB) and ***b*** is the Least Significant Bits (LSB). The transmitter encodes ***s*** into a constellation label using a signal shaping algorithm. One of the well-known signal shaping algorithms, shell mapping, is used in the V.34 telephone-line modem and its successors. In shell mapping, the region (shell) number is sorted according to the associated energy, K-bit data is mapped to one of N shell indices with the possible lowest number. Since only 2^K least energy shells are used, total energy must decrease with shell mapping.

The other well-known signal shaping algorithm, trellis shaping, is associated with the use of an error-correcting code. A block diagram of the algorithm is shown in Figure 4. In the algorithm, N consecutive symbols correspond to code words of length N, and the code symbols are taken from an M-ary alphabet; the cardinality of the code is 2^K. A K-bit data is transformed into a code word using the shaping algorithm described below. To minimize the power, the code must be selected from the innermost region possible. In the receiver, the code word is decoded to the original K-bit data. In the arithmetic representation of shaping, let $\boldsymbol{G}$ and $\boldsymbol{H}$ be the $(N\text{-}K)\text{x}N$ generator matrix of the error correcting code and the $K\text{x}N$ parity check matrix, such that $\boldsymbol{GH}^{\mathrm{T}}=\mathbf{0}_{(N\text{-}K)\text{x}K}$, where is $\boldsymbol{H}^{\mathrm{T}}$ the transpose of $\boldsymbol{H}$ and $\mathbf{0}$ is the null matrix of the given dimension. In the representation, K-bit data $\boldsymbol{s}$ is considered as a syndrome, and is mapped to code word $\boldsymbol{z}$ of length N as follows:

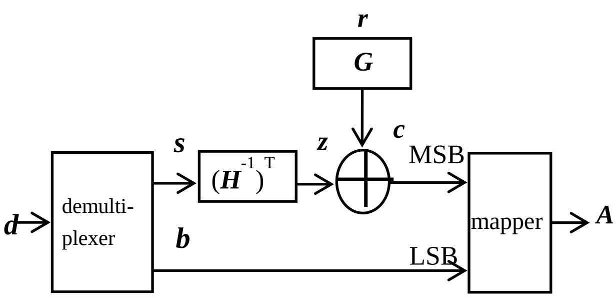

(a) Transmitter

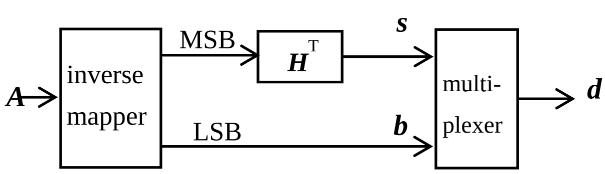

(b) Receiver

Figure 4. Trellis shaping system

$$\boldsymbol{s}=\boldsymbol{zH}^{\mathrm{T}}. \quad (2)$$

Provided the left inverse of $\boldsymbol{H}^{\mathrm{T}}$ is $(\boldsymbol{H}^{-1})^{\mathrm{T}}$, i.e. $(\boldsymbol{H}^{-1})^{\mathrm{T}}\boldsymbol{H}^{\mathrm{T}}=\mathbf{I}_{K\text{x}K}$, the matrix can be viewed as a coset representative generator. Using syndrome $\boldsymbol{s}$, coset representative $\boldsymbol{z}$ is expressed as follows:

$$\boldsymbol{z}=\boldsymbol{s}(\boldsymbol{H}^{-1})^{\mathrm{T}}. \quad (3)$$

Therefore, any code word $\boldsymbol{c}=\boldsymbol{rG}$ generates an all-zero syndrome $\boldsymbol{s}$, where $\boldsymbol{r}$ is a $(N\text{-}K)$bit code, since $\boldsymbol{s}=\boldsymbol{cH}^{\mathrm{T}}=\boldsymbol{rGH}^{\mathrm{T}}=\boldsymbol{r}\mathbf{0}=\mathbf{0}$. This means that syndrome $\boldsymbol{s}$ of coset representative $\boldsymbol{z}$ does not change with the addition of any code word, since

$$(\boldsymbol{z}+\boldsymbol{c})\boldsymbol{H}^{\mathrm{T}}=\boldsymbol{zH}^{\mathrm{T}}+\boldsymbol{cH}^{\mathrm{T}}=\boldsymbol{s}+\mathbf{0}=\boldsymbol{s}, \quad (4)$$

where + means modulo-two addition.

Provided the Binary Coded Decimal (BCD) of coset member $\boldsymbol{z}+\boldsymbol{c}$ is given to the region as its label in the constellation, the desired coset member with minimum power can be found by varying $\boldsymbol{r}$. To find a valid code word with minimum power, the trellis diagram is used with the Viterbi algorithm, the trellis shaping approach. As an example of the block code, each code word is described as a path in the trellis diagram [22], where the trellis shaping algorithm searches for the desired code using signal power as a metric. In this way, the smallest possible BCD of $\boldsymbol{z}+\boldsymbol{c}$ is selected from the constellation in Figure 2.

4. Signal Shaping in Constellation Sharing

In the PON system described in Figure 1, the existing OLT and ONU use OOK coding, which require extinction ratios as large as 20 dB to realize low BER. On the other hand, the large extinction ratio makes it difficult to discriminate the phase information among different symbols, when they are OFF. This paper introduces a signal shaping algorithm to solve this problem.

Provided the constellation is divided into two regions, i.e. M=2, and the data word $\boldsymbol{d}$ is the connection of $\boldsymbol{s}$ and $\boldsymbol{b}$, $\boldsymbol{s}$ and $\boldsymbol{b}$ are expressed as region number (radius) and argument (phase) in the constellation, respectively. In other words, $\boldsymbol{s}$ and $\boldsymbol{b}$ denote the OOK signals and PSK signals, respectively. In the shell mapping approach, $\boldsymbol{s}$ is encoded to $\boldsymbol{s'}$, where each bit of $\boldsymbol{s'}$ is used as a new MSB of the transmitted symbol, and the parameters are set to K=2 and N=3. Shell mapping defines the one to one mapping of $\boldsymbol{s}$ to $\boldsymbol{s'}$ as follows; the values of $\boldsymbol{s}$ such as (0,0), (0,1), (1,0), and (1,1) are encoded to $\boldsymbol{s'}$ of (0,1,1), (1,0,1), (1,1,0), and (1,1,1), respectively. The result maximizes the Euclid distance among the symbols by mapping "1" to the outer region of the constellation. Since commercial electric power is supplied to the OLT and ONU in the PON network, power consumption is a small factor in designing the system.

In the trellis shaping approach, the shaping algorithm selects the largest BCD of coset member so that the symbols carry the largest power and maximize the Euclid distance among symbols in Figure 2. As an example, the binary (7, 4) hamming code can be applied to the shaping algorithm. Its generator matrix $\boldsymbol{G}$ and the respective parity-check matrix $\boldsymbol{H}$ are given as

$$\boldsymbol{G}=\begin{bmatrix}1 & 1 & 0 & 1 & 0 & 0 & 0\\ 0 & 1 & 1 & 0 & 1 & 0 & 0\\ 0 & 0 & 1 & 1 & 0 & 1 & 0\\ 0 & 0 & 0 & 1 & 1 & 0 & 1\end{bmatrix}, \quad (5)$$

$$\boldsymbol{H} = \begin{bmatrix} 1 & 0 & 1 & 1 & 1 & 0 & 0 \\ 0 & 1 & 0 & 1 & 1 & 1 & 0 \\ 0 & 0 & 1 & 0 & 1 & 1 & 1 \end{bmatrix}. \quad (6)$$

The corresponding left inverse of $\boldsymbol{H}^T$ is [22]

$$\left(\boldsymbol{H}^{-1}\right)^T = \begin{bmatrix} 1 & 0 & 0 & 0 & 0 & 0 & 0 \\ 0 & 1 & 0 & 0 & 0 & 0 & 0 \\ 0 & 0 & 0 & 0 & 0 & 0 & 1 \end{bmatrix}. \quad (7)$$

In this code, the coset representatives are 7-bit code, and their number is $2^{(7-4)}=8$. The binary data of OOK is divided into plural sets of 3-bit data, which are described as $\boldsymbol{s}$, and the coset representative $\boldsymbol{z}$ is derived from equation (3). Based on the shaping algorithm described above, $\boldsymbol{z}+\boldsymbol{c}$ is provided to the mapper, i.e. OOK modulator. Note that data $\boldsymbol{b}$ encoded with PSK signaling is not passed through the signal shaping algorithm.

5. OptSim and MATLAB Co-simulation

Simulations were carried out by using OptSim and MATLAB software. OptSim is an advanced optical communication system simulation package designed for professional engineering and emerging optical systems [23]. In this work, signal shaping is carried out by MATLAB while OptSim simulates the optical devices, such as continuous wave (CW) laser, amplitude modulator, Raised Cosine filter, optical fiber, and Positive-Intrinsic-Negative (PIN) receiver. The network configuration shown in Figure 1 is assumed, where the OLT is connected to three ONUs via a 1:4 optical splitter and standard single mode fiber. The modulation format is shown in Figures 5(a) and (b), where one bit signal (MSB), denoted by $\boldsymbol{s}$, is modulated using OOK, and the amplitude of the signal expresses the bit. In contrast, the phase represents two bits by using QPSK or three bits by 8PSK, as shown in Figures 5(a) and(b), respectively.

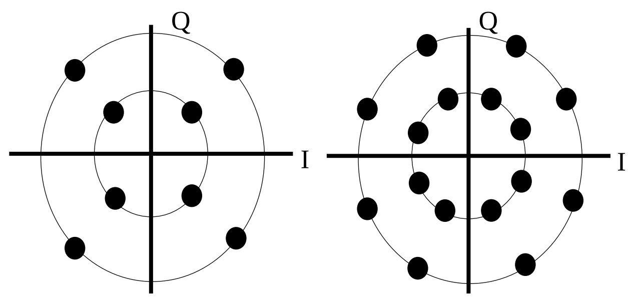

(a) OOK and QPSK (b) OOK and 8-PSK

Figure 5. Constellation

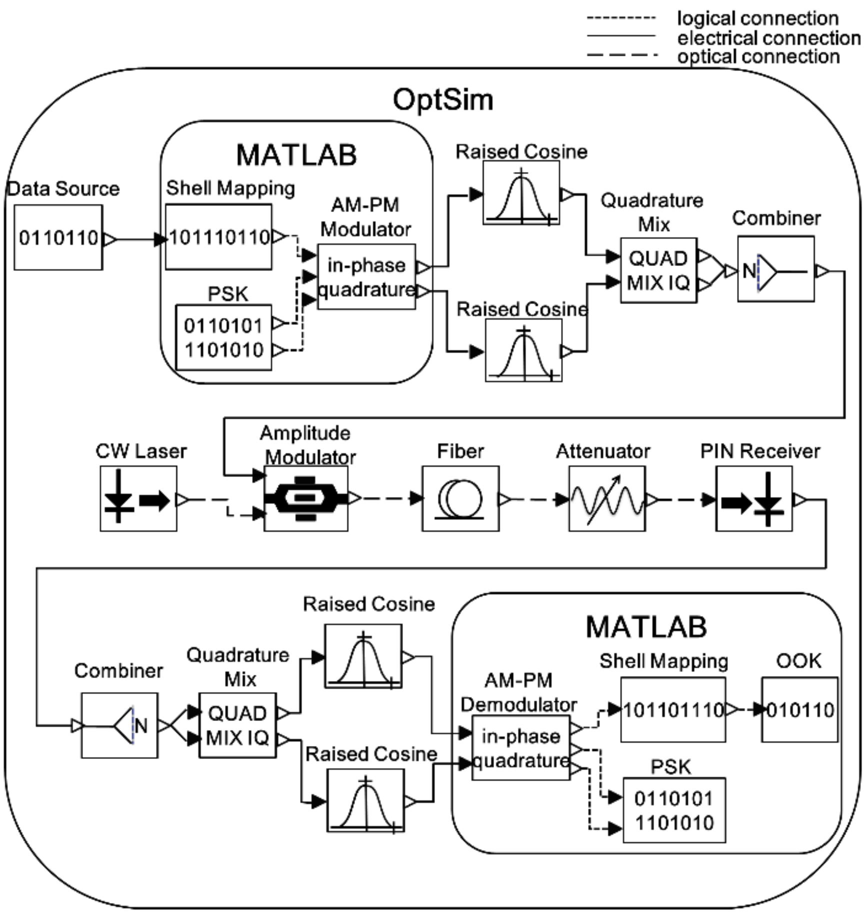

Figure 6. Simulation setup schematics

Six simulations were performed: OOK+QPSK with shell mapping, OOK+QPSK with trellis coding, OOK+QPSK without shaping, OOK+8PSK with shell mapping, OOK+8PSK with trellis shaping and OOK+8PSK without shaping. As one example, Figure 6 shows the simulation setup schematics for OOK+QPSK with shell mapping. The values of important parameters are shown in Table 1.

Table 1. Values of simulation parameters

Modulation format	AM_PM(OOK+QPSK) AM_PM(OOK+8PSK)
Symbol rate [Gsymbol/s]	1
The number of symbols [symbol]	2.5×10^4
Fiber length [km]	1
Transmission power [dBm]	-3
Extinction ratio [dB]	20

A 1 Gsymbol/s OOK+PSK signal is launched into 1km of standard single mode fiber. The OOK signal is shell mapped using a program written in MATLAB. The modulation uses orthogonal carriers to transport the phase and amplitude information of the modulated bits. The in-phase and quadrature components go through the raised cosine filter to reduce the inter-symbol interference, and are combined by the quadrature mixer. The combined signals are input to the optical amplitude modulator, and the modulated optical signals are launched into the optical fiber. After transmission over 1km of fiber, the optical signal is filtered and detected by a PIN photodiode which is preceded by an attenuator. Synchronous detection is used to extract in-phase and quadrature phase components from the output of the PIN photodiode. Finally, the received OOK+PSK signals are converted into PSK and OOK signals by MATLAB, which also realizes the receiver side processing for signal shaping.

6. Simulation Results and Discussion

This section describes the two-dimensional distribution of the signals and BER characteristics to show the effect of signal shaping.

6.1. Two-Dimensional Distribution of Signals

As described above, the MSB of the data is modulated by OOK and is shaped by shell mapping or trellis shaping; the other bits are PSK modulated. The distributions of the transmitted symbols are shown in Figures 7(a) to (d). The height of the vertical bar shows the probability density of each signal. In these figures, the probability of the signals in the outer region is three times larger than that in the inner region. This implies that the probability of the signals in the inner region is quite low, which minimizes the BER degradation of the PSK signals.

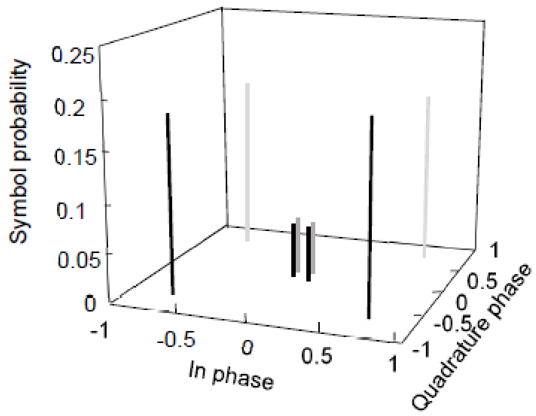

(a) OOK+QPSK with shell mapping

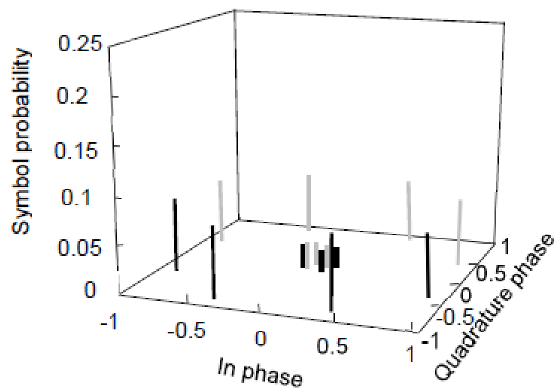

(b) OOK+8PSK with shell mapping

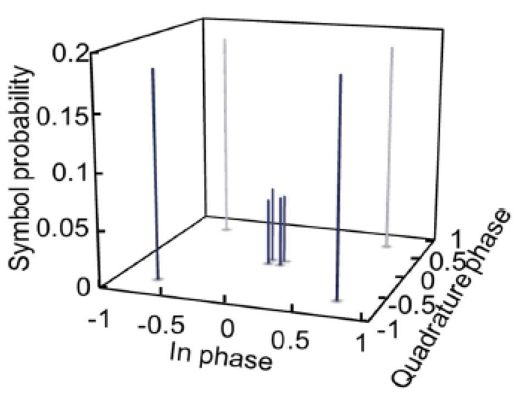

(c) OOK+QPSK with trellis shaping

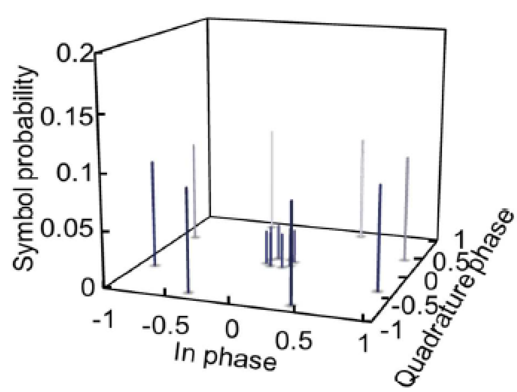

(d) OOK+8PSK with trellis shaping

Figure 7. Symbol probability in constellation sharing

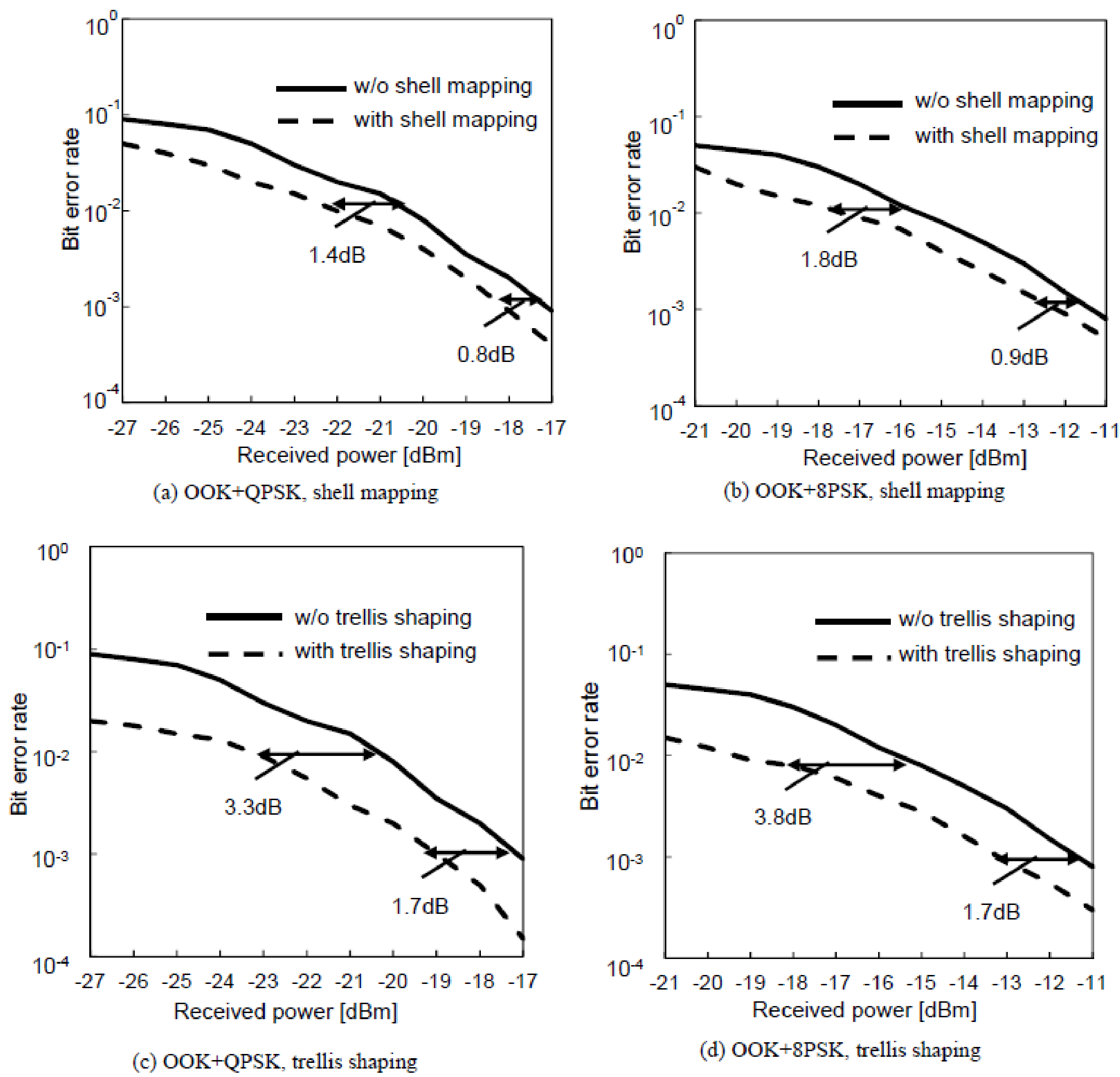

Figure 8. BER of PSK signals with constellation sharing

6.2. BER Characteristics of PSK Signal

Using the simulation configuration described in Section 5, the BER characteristics of QPSK and 8PSK signals are measured with shell mapping or trellis shaping in constellation sharing. Additionally, the BER without signal shaping is also derived as a reference. Regarding shell mapping, the result of QPSK+OOK is shown in Figure 8(a), and that of OOK+8PSK is shown in Figure 8 (b), respectively. These figures show that OOK+QPSK with shell mapping achieves the received power gain of 1.4 dB at BER of 10^{-2} and 0.8 dB at BER of 10^{-3}. The received power gain values of OOK+8PSK in this environment is 1.8 dB at BER of 10^{-2} and 0.9 dB at BER of 10^{-3}. On the other hand, with trellis shaping, the result of QPSK+OOK is shown in Figure 8(c), and that of OOK+8PSK is shown in Figure 8(d), respectively. These figures show that the received power gain is 3.3 dB at the BER of 10^{-2} and 1.7 dB at BER of 10^{-3} in the constellation sharing of OOK and QPSK, and the gain is 3.8 dB at BER of 10^{-2} and 1.7 dB at BER of 10^{-3} in OOK+8PSK. These results show the improvement in BER possible with constellation sharing of OOK and PSK where an existing PON coexists the next generation system technology.

6.3. Discussion

As described in section 2, constellation sharing reduces the Euclidian distance of the PSK symbols and degrades the BER of the PSK signals, when the symbols are OFF. According to the proposal of the use of signal shaping, the MSB of the data is modulated by OOK and is shaped by shell mapping or trellis shaping; the other bits are PSK modulated. The shaping algorithm selects the symbols in the outer region so that the symbols carry the largest power and maximize the Euclid distance among symbols. In fact, the probability of the signals in the outer region is three times larger than that in the inner region, as discussed in section 6.1. This shows that the probability of the signals in the inner region is quite low, which minimizes the BER degradation of the PSK signals. The measured BER characteristics show the improvement by applying the shell mapping and trellis shaping algorithms, as discussed in section 6.2.

The above results clarified that both shaping algorithms, shell mapping and trellis shaping, increase the distribution of the signals in the outer region of OOK+PSK constellation sharing. In addition, the BER characteristics of PSK improve by more than 1 dB with shell mapping compared to that without shaping, and the improvement is more than 3 dB with trellis shaping. These results show that trellis shaping offer larger BER improvement than that shell mapping. One of the disadvantages of signal shaping is that the increase in the code rate reduces the signal efficiency. For example, use of the (7, 4) hamming code expands data s of 3 bits to $z+c$, i.e. 7 bits, so the OOK signal efficiency is 0.43. This implies that signal shaping improves the BER of PSK signals at the cost of OOK signal efficiency. Regarding the total efficiency of OOK+4PSK, it is 0.8. In the environment of next generation PON and the existing system co-existence, since PSK signals represent more bits than OOK, the former's improvement far outweighs the latter's penalty.

7. Conclusions

This paper compared shell mapping and trellis shaping for symbol mapping to improve the transmission characteristics of the next generation Passive Optical Network (PON) system when co-existing with the conventional one. The mapping proposal solves one of the most critical problems; the small Euclid distance of the PSK signals in a constellation shared by OOK and PSK. The conventional system uses OOK for its simplicity, while the next generation uses advanced techniques such as PSK.

This paper described the configuration, operation principle, and co-simulation architecture of MATLAB and OptSim for clarifying the improvement achieved by the mapping proposal. The co-simulation clarified the BER characteristics of the PSK improve by more than 1 dB with shell mapping compared to that without shaping, and the improvement is more than 3 dB with trellis shaping. These results show that trellis shaping offers larger BER improvement than shell mapping. The proposal will make the co-existence of the existing PON and the next generation technology practical.

ACKNOWLEDGEMENTS

This work was supported by JSPS KAKENHI Grant (C) Number 26420377 and by the Nanzan University Pache Research Subsidy I-A-2 for the 2016 Academic year, for which the authors would like to express their thanks.

REFERENCES

[1] T. Koonen, "Trends in optical access and in building networks," Proc. 2008 Eur. Conf. Opt. Commun. (ECOC), pp. 1-31, We2. A.1, 2008.

[2] D. Qian, J. Yu, J. Hu, L. Zong, L. Xu, and T. Wang, "8x11.5 Gbps OFDM transmission over 1000 km SSMF using conventional DFB lasers and direct-detection," IEEE Electron. Lett., vol. 44, no. 3, pp. 223-225, May 2008.

[3] P. Chanclou, J. P. Lanquetin, S. Durel, F. Saliou, B. Landousies, N. Genay, and Z. Belfqih, "Investigation into optical technologies for access evolution," Proc. 2008 IEEE/OSA Opt. Fiber Commun. Conf (OFC/NFOEC), pp. 1-3, OWH1, 2008.

[4] ITU-T Rec. G.987.2, "10-Gigabit-Capable Passive Optical Networks (XG-PON): Physical Media Dependent (PMD) Layer Specification," Oct. 2010.

[5] N. Cvijetic et al., "Software-defined heterogeneous 100Gb/s mobile backhaul with 1000+ per-fiber cell counts," Opto-Electronics and Commun. Cof. '12, Technical Digest, PDP1-2, 2012.

[6] X. Yin, F. Blanche, B. Moeneclaey, J. van Kerrebrouck, R. Brenot, G. Qiu, Coudyzer, M. Achouche, X. Qui, and J. Bauwelinck, "40-Gb/s TDM-PON Downstream with Low-cost EML Transmitter and 3-Level Detection APD Receiver," Proc. OFC 2016, Tu3C.1, Anaheim, USA, 2016.

[7] S. Yin, D van Veen, V. Houtsma, and P. Vetter, "Investigation of Symmetrical Optical Amplified 40 Gbps PAM-4/Duobinary TDM-PON using 10G Optics and DSP," Proc. OFC 2016, Tu3C.2, Anaheim, USA, 2016.

[8] M. Fujiwara, R. Koma, K. Suzuki, and A. Otaka, "Compact Bi-directional EDFAs to Support Extended Power Budget Class of TWDM-PON", Proc. ECOC2015, Mo.4.4.3, Valencia, Spain, 2015.

[9] S. Shimizu, Y. Kado, S. Kinoshita, N. Wada, and K. Kitayama, "Long-Reach 10G-EPON over Optical Packet/ Circuit Integrated Backbone Networks: Test-Bed Demonstration," Proc. ECOC2015, Mo.4.4.4, Valencia, Spain, 2015.

[10] D. Qian, N. Cvijetic, J. Hu, and T. Wang, "108 Gb/s OFDMA-PON with polarization division multiplexing and direct detection," Proc. 2009 IEEE/OSA Opt. Fiber Commun. Conf. (OFC/NFOEC), pp. 1-2, PDPD5, 2009. "PDCA12-70 data sheet," Opto Speed SA, Mezzovico, Switzerland.

[11] D. Qian, N. Cvijetic, J. Hu, and T. Wang, "108 Gb/s OFDMA-PON with polarization multiplexing and direct detection," IEEE J. Lightw. Technol., vol. 28, no. 4, pp. 484-493, Feb. 2010. J. Padhye, V. Firoiu, and D. Towsley, "A stochastic model of TCP Reno congestion avoidance and control," Univ. of Massachusetts, Amherst, MA, CMPSCI Tech. Rep. 99-02, 1999.

[12] T. Duong, N. Genay, P. Chanclou, B. Charbonnier, A. Pizzinat, and R. Brenot, "Experimental demonstration of 10Gbit/s upstream transmission by remote modulation of 1 GHz RSOA using adaptively modulated optical OFDM for WDM-PON single fiber architecture," Proc. 2008 Eur. Conf. Opt. Commun. (ECOC), pp. 1-2, We.1.F.4, 2008.

[13] J. Armstrong, "OFDM for optical communications," J. Lightw. Technol., vol. 27, no. 3, pp. 189-204, Jan. 2009.

[14] N. Iiyama, S. Y. Kim, T. Shimada, S. Kimura, and N. Yoshimoto, "Co-existent downstream scheme between OOK and QAM signals in an optical access network using software-defined technology," IEEE/OSA Opt. Fiber Commun. Conf (OFC/NFOEC) 2012, OSA Technical Digest, paper JTh2A.53, 2012.

[15] N. Yoshimoto, J. Kani, S. Y. Kim, N. Iiyama, and J. Terada, "DSP-based optical access approaches for enabling NG-PON2 systems," IEEE Commun. Magazine, vol. 51, pp. 58-64, March 2013.

[16] R. Koma, M. Fujiwara, J. Kani, K. Suzuki, and A. Otaka, "Wide Dynamic Range Burst-Mode Digital Coherent Detection Using Fast ALC-EDFA and Pre-Calculation of FIR Filter Coefficients," Proc. OFC 2016, M3C.6, Anaheim, USA, 2016.

[17] H. Saito, N. Minato, S. Kobayashi, and H. Tamai, "Adaptive Bandwidth Allocation for WDM/OFDM-PON-based Elastic Lambda Aggregation Network," Proc. OFC 2016, Th3C.2, Anaheim, USA, 2016.

[18] D. van Veen, V. Houtsma, and H. Chow, "Demonstration of Symmetrical 25 Gbps Quaternary PAM/Duobinary TDM-PON Upstreamwith Multilevel Interleaving of Users," Proc. ECOC2015, Mo.3.4.1, Valencia, Spain, 2015.

[19] S. Straullu, P. Savio, A. Nespola, J. Chang, V. Ferrero, R. Gaudino, and S. Abrate, "Demonstration of Upstream WDM+FDMA PON and Real Time Implementation on an FPGA Platform," Proc. ECOC2015, Mo.3.4.3, Valencia, Spain, 2015.

[20] G. D. Forney Jr., "Trellis shaping," IEEE Trans. Inform. Theory, vol. 38, pp. 281-300, March 1992.

[21] I. S. Morrison, "Trellis shaping applied to reducing the envelope fluctuations of MQAM and band-limited MPSK," Proc. Int. Conf. Digital Satellite Commun. (ICDSC '92), pp. 143-149, May 1992.

[22] R. F. H. Fischer, *Precoding and signal shaping for digital transmission*, IEEE Press, 2002.

[23] *OptSim User Guide*, Synopsys, Inc., 2013.